SAND2012-10761P

Solar Glare Hazard Analysis Tool (SGHAT) User's Manual v. 1.0

Clifford K. Ho and Cianan A. Sims
Sandia National Laboratories
(505) 844-2384, ckho@sandia.gov
November 30, 2012

Contents

1. Requirements

- Use of this software requires the latest version of one of the following free web browsers: Mozilla Firefox or Google Chrome.
- The Solar Glare Hazard Analysis Tool (SGHAT) can be accessed by registering at www.sandia.gov/glare. SGHAT is located at https://share.sandia.gov/phlux/sghat.

2. Introduction

With growing numbers of solar energy installations throughout the United States, glare from photovoltaic (PV) arrays and concentrating solar systems has received increased attention as a real hazard for pilots, air-traffic control personnel, motorists, and others. Sandia has developed a web-based interactive tool that provides a quantified assessment of (1) when and where glare

will occur throughout the year for a prescribed solar installation, and (2) potential effects on the human eye at locations where glare occurs.

The Solar Glare Hazard Analysis Tool (SGHAT) employs an interactive Google map where the user can quickly locate a site, draw an outline of the proposed PV array, and specify observer locations or paths. Latitude, longitude, and elevation are automatically recorded through the Google interface (see Figure 1), providing necessary information for sun position and vector calculations. Additional information regarding the orientation and tilt of the PV panels, reflectance, environment, and ocular factors are entered by the user.

If glare is found, the tool calculates the retinal irradiance and subtended angle (size/distance) of the glare source to predict potential ocular hazards ranging from temporary after-image to retinal burn. The results are presented in a simple, easy-to-interpret plot that specifies when glare will occur throughout the year, with color codes indicating the potential ocular hazard. The tool can also predict relative energy production while evaluating alternative designs, layouts, and locations to identify configurations that maximize energy production while mitigating the impacts of glare.

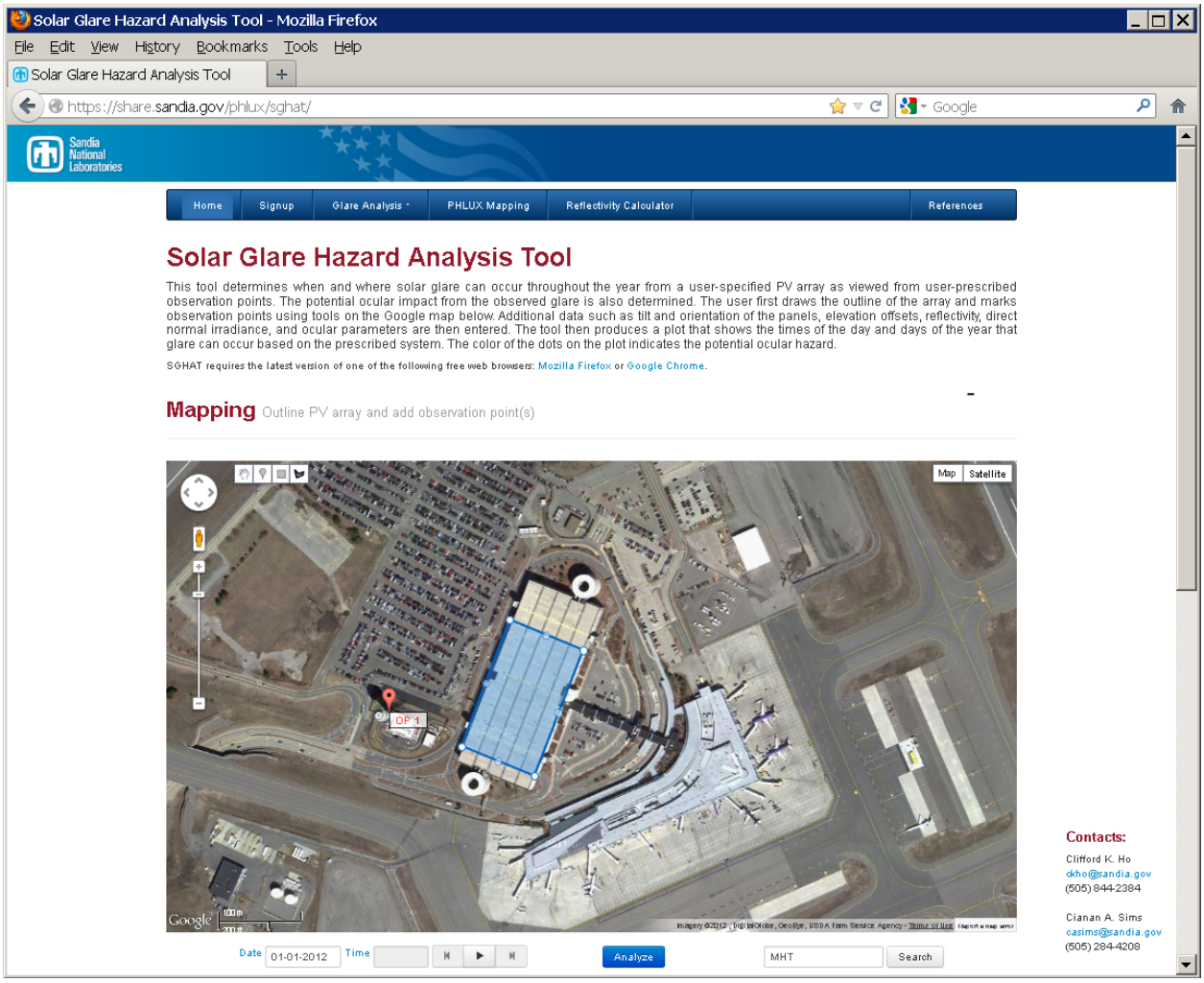

Figure 1. Screen image of SGHAT starting page with Google Map interface.

3. Mapping PV Arrays and Observation Points

On the starting page, a brief introduction to the tool is provided along with a Google map (see Figure 1). The user first identifies the location and outline of a PV array. Then, observation points (one or more) can be selected for the glare analysis.

3.1 Locating and Outlining a PV Array

- Beneath the Google map, enter the city, airport, zip code, etc. in the search field to find the appropriate location
  - Use the zoom features to adjust the scale
  - Use the "Satellite" mode to view buildings and other structures for reference
- Click on the rectangle or polygon tool to outline the footprint of the PV array on the map

  - For the rectangle tool, click and drag to draw a rectangular shape
  - For the polygon tool, click on the vertices of the desired footprint to create a polygon. Click on the first point again to close the polygon.
  - The elevation of the PV array above ground level (e.g., if it is located on a rooftop) can be specified in the data entry fields (see Section 4).
  - Use the hand tool to translate the map up/down or side to side

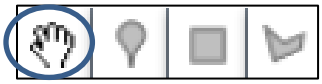

  - An outline can be cleared by clicking on "Clear Array" in the data entry section below the map or by simply redrawing a new outline

3.2 Locating Observation Points

- Use the observation marker to select locations on the map where you would like to analyze solar glare (reflected from the prescribed PV array)

  - The elevation of the observation point above ground level (e.g., from an air traffic control tower, plane) can be specified in the data entry fields (see Section 4)
  - Multiple observation point can be specified (each observation point is labeled OP1, OP2 etc.)
  - The scale in the lower left-hand corner of the Google map is useful for spacing observation points relative to other points or objects
  - Observation points can be cleared by clicking on "Clear Observations" in the data entry section below the map or by selecting the hand tool and right clicking on an observation point

4. Data Entry

Beneath the Google map, data can be entered to prescribe features of the PV array, observation points, solar irradiance, and ocular conditions in the "Data and Coordinates" tab.

- *Analysis Name:* Name the analysis. Multiple analyses can be performed and stored in the Results section.
- *Orientation of array:* Specify the orientation of the array in degrees, measured clockwise from due north. Modules facing east would have an orientation of 90°, and modules facing south would have an orientation of 180°.
- *Tilt of solar panels:* Specify the tilt (elevation angle) of the modules in degrees, where 0° is facing up and 90° is facing horizontally.
- *Height of solar panels:* Specify height (m) of modules above ground level.
- *Rated power:* Specify the rated power (kW) of the PV system. This is used to calculate the maximum annual energy produced (kWh) from the system in the prescribed configuration (assuming clear sunny days). This is useful for comparing alternative configurations to determine which one has the maximum energy production.
- *Reflectivity of PV module:* Specify the solar reflectance of the PV module. Although near-normal reflectance of PV glass (e.g., with antireflective coating) can be as low as ~3%, the reflectance can increase as the incidence angle of the sunlight increases (glancing angles). Based on evaluation of several different PV modules, a reflectance of 10% appears reasonable.
- *Slope error:* This parameter specifies the amount of scatter that occurs from the PV module. Mirror-like surfaces that produce specular reflections will have a slope error closer to zero, while rough surfaces that produce more scattered (diffuse) reflections have higher slope errors. Based on observed glare from different PV modules, an RMS slope error of ~10 mrad (which produces a total reflected beam spread of 0.13 rad or 7°) appears to be a reasonable value.
- *Subtended angle of the sun:* The average subtended angle of the sun as viewed from earth is ~9.3 mrad or 0.5°.
- *DNI:* Direct Normal Irradiance (W/m^2). On a clear sunny day at solar noon, the DNI is ~1,000 W/m^2.
- *Transmission coefficient:* The ocular transmission coefficient accounts for radiation that is absorbed in the eye before reaching the retina. A value of 0.5 is typical [1, 2].
- *Pupil diameter:* Diameter of the pupil (m). The size impacts the amount of light entering the eye and reaching the retina. Typical values range from 0.002 m for daylight-adjusted eyes to 0.008 m for nighttime vision [1, 2].
- *Eye focal length:* Distance between the nodal point (where rays intersect in the eye) and the retina. This value is used to determine the projected image size on the retina for a given subtended angle of the glare source. Typical value is 0.017 m [1, 2].

- *Time interval:* Specify the time step for the glare analysis. The sun position will be determined at each time step throughout the year. A time step of 1 minute yields excellent resolution.
- *Data output:* Specify if downloadable data that can be read in Excel is desired (takes a bit longer for the analysis). Even if no output is selected, results can be viewed in the "Results" tab.
- *Height above ground (under Observation Points):* Specify the height of the observation point above ground. Google Maps automatically determines the ground elevation (above mean sea level) based on the selected points, so the specified height should be the elevation above ground level.

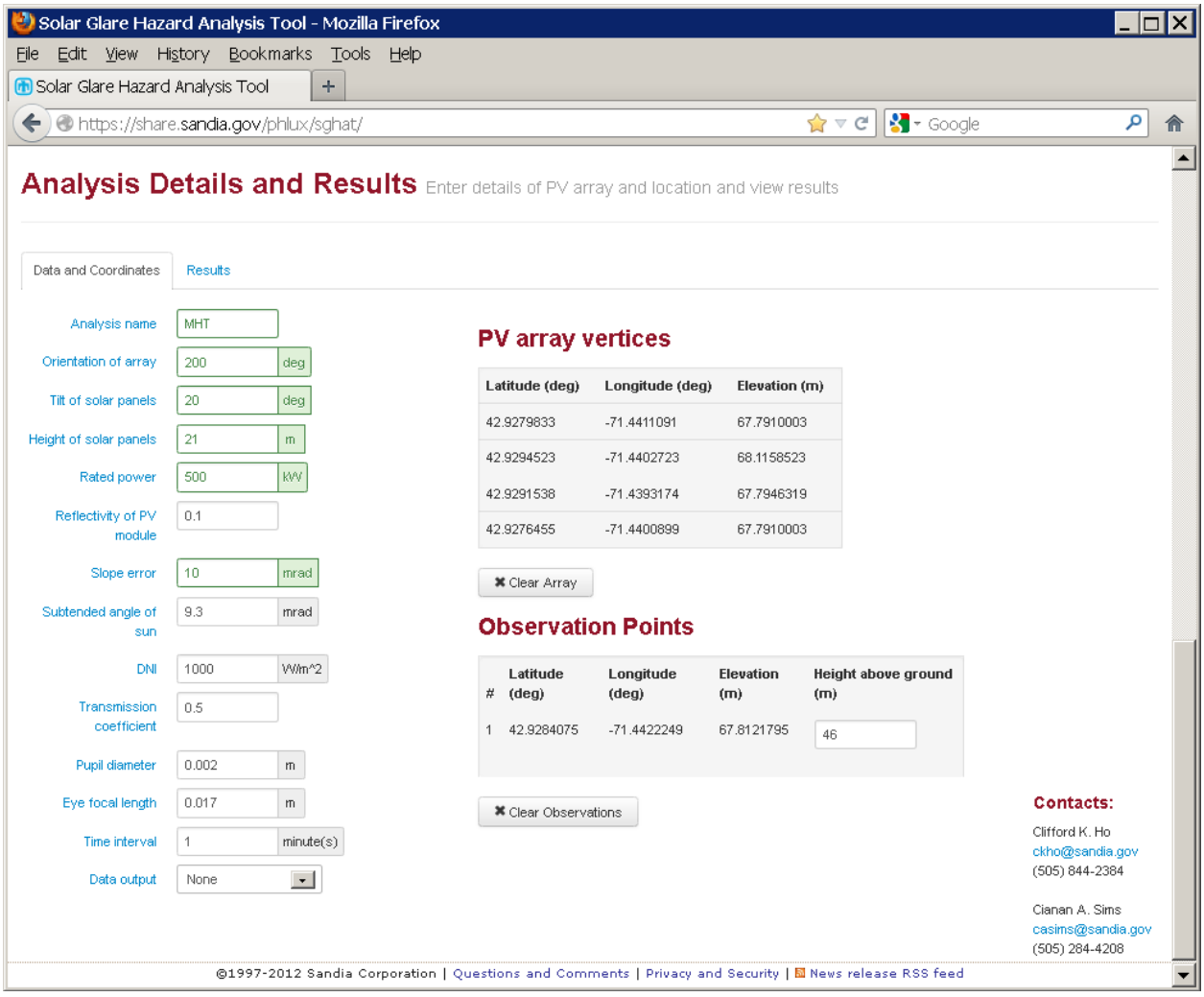

Figure 2. Screen image of data entry fields.

5. Evaluating Results

After entering the PV array, observation points, and data in the previous sections, click the "Analyze" button below the Google map (see Figure 1). An analysis box should appear indicating the status of the run (Figure 3).

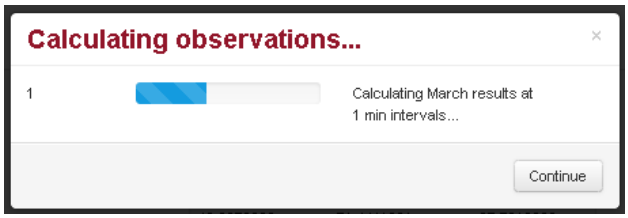

Figure 3. Screen image showing status of analysis.

When the analysis is complete, click on "Continue" and then click on the "Results" tab. A summary of the input parameters is shown for the current analysis, along with the annual energy production and Glare Occurrence Plot (Figure 4). On the right side of the screen image shown in Figure 4, multiple analyses are shown and can be selected to view and compare results.

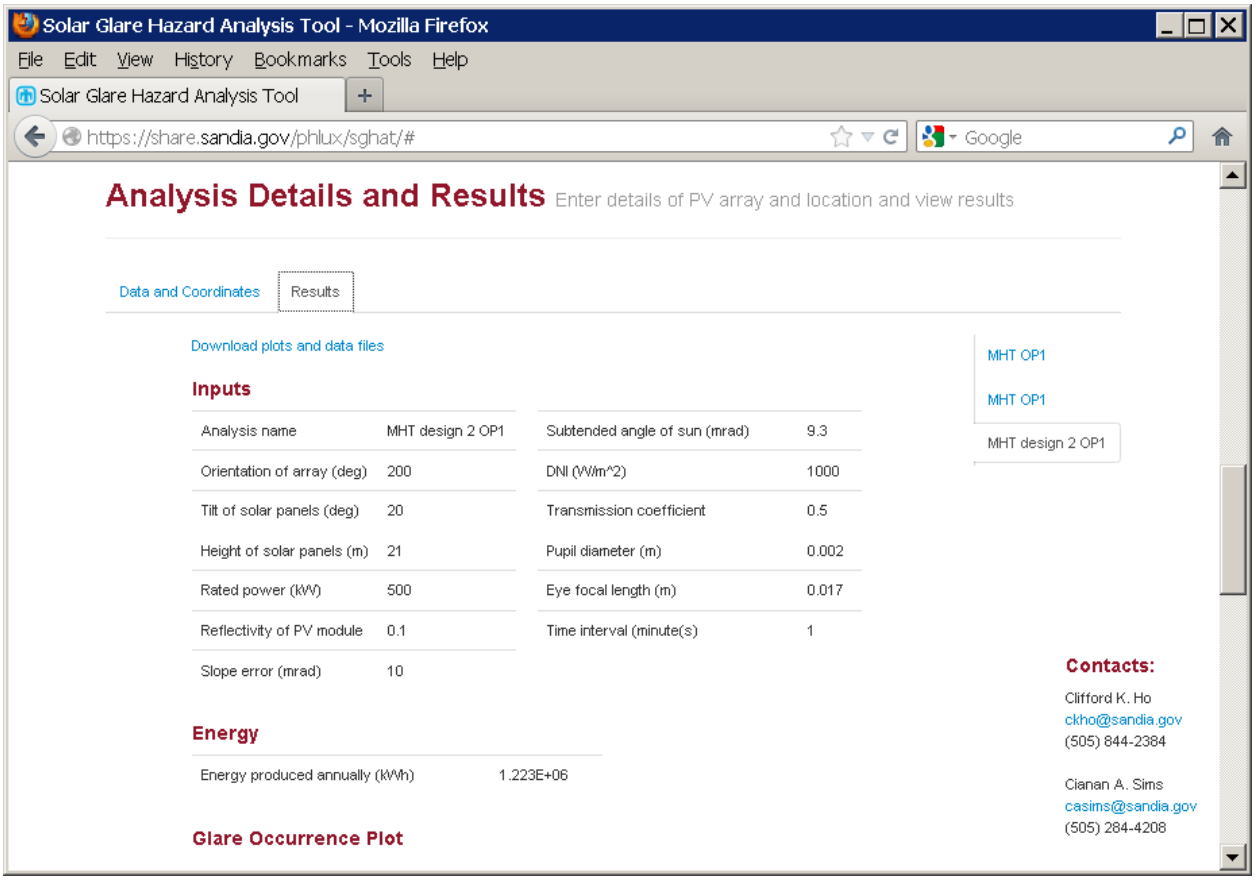

Figure 4. Screen image of results section.

The Glare Occurrence Plot shows when glare can occur (as viewed from the prescribed observation point) throughout the year. The color of the dots indicates the potential ocular hazard [1] as shown in Figure 5. In the example shown in Figure 5, glare is predicted to be visible from the prescribed observation point during the morning from January to November for ~30 – 40 minutes. Based on the conditions of the site and system entered by the user, a potential for temporary after-image exists.

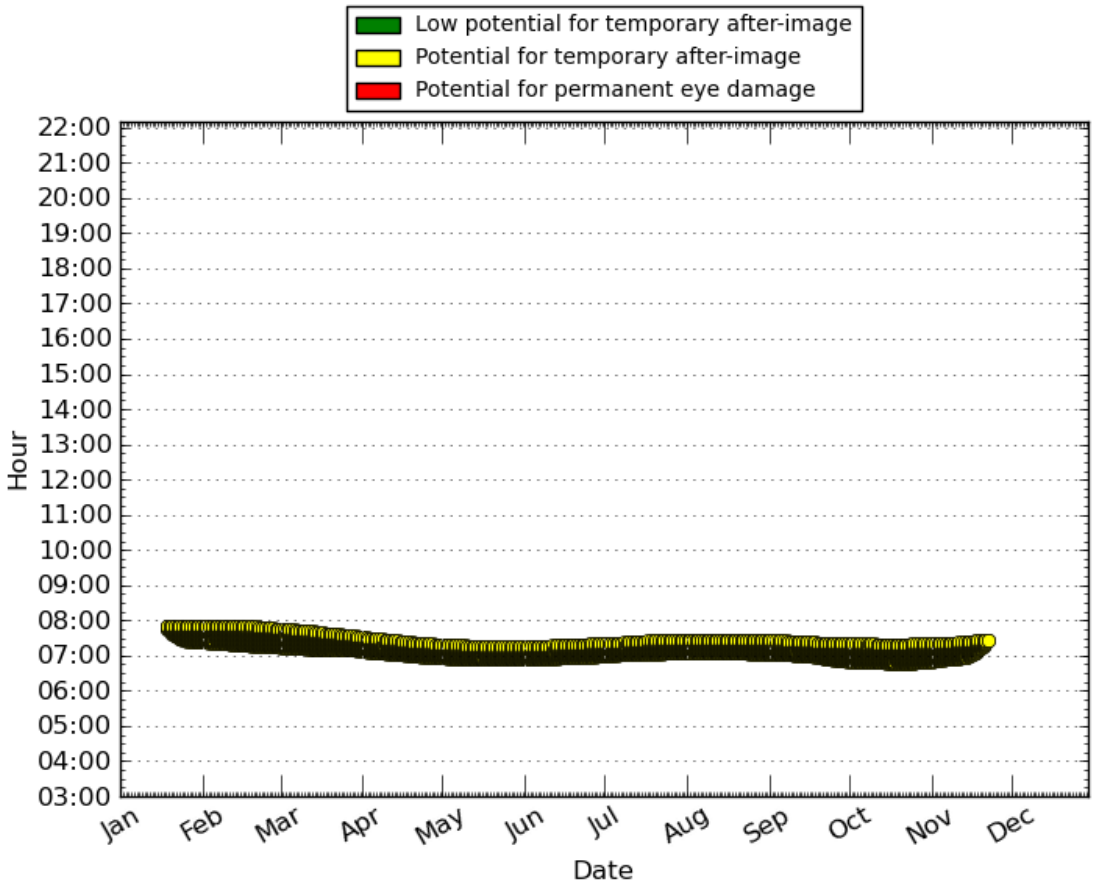

Figure 5. Glare occurrence plot showing when glare can occur (time and date) and the potential for ocular impact (represented by the color of the dots). Times are shown in Standard Time (during Daylight Savings Time, add one hour).

6. Case Study and Example

We include a sample analysis of the Manchester-Boston Regional Airport (MHT), which has experienced glare from PV panels that were installed on the roof of a parking garage near the air traffic control tower. The blue highlighted area in Figure 6 is drawn by the user to denote the location of the PV array. The red marker indicates the location of the observer in the air traffic control tower.

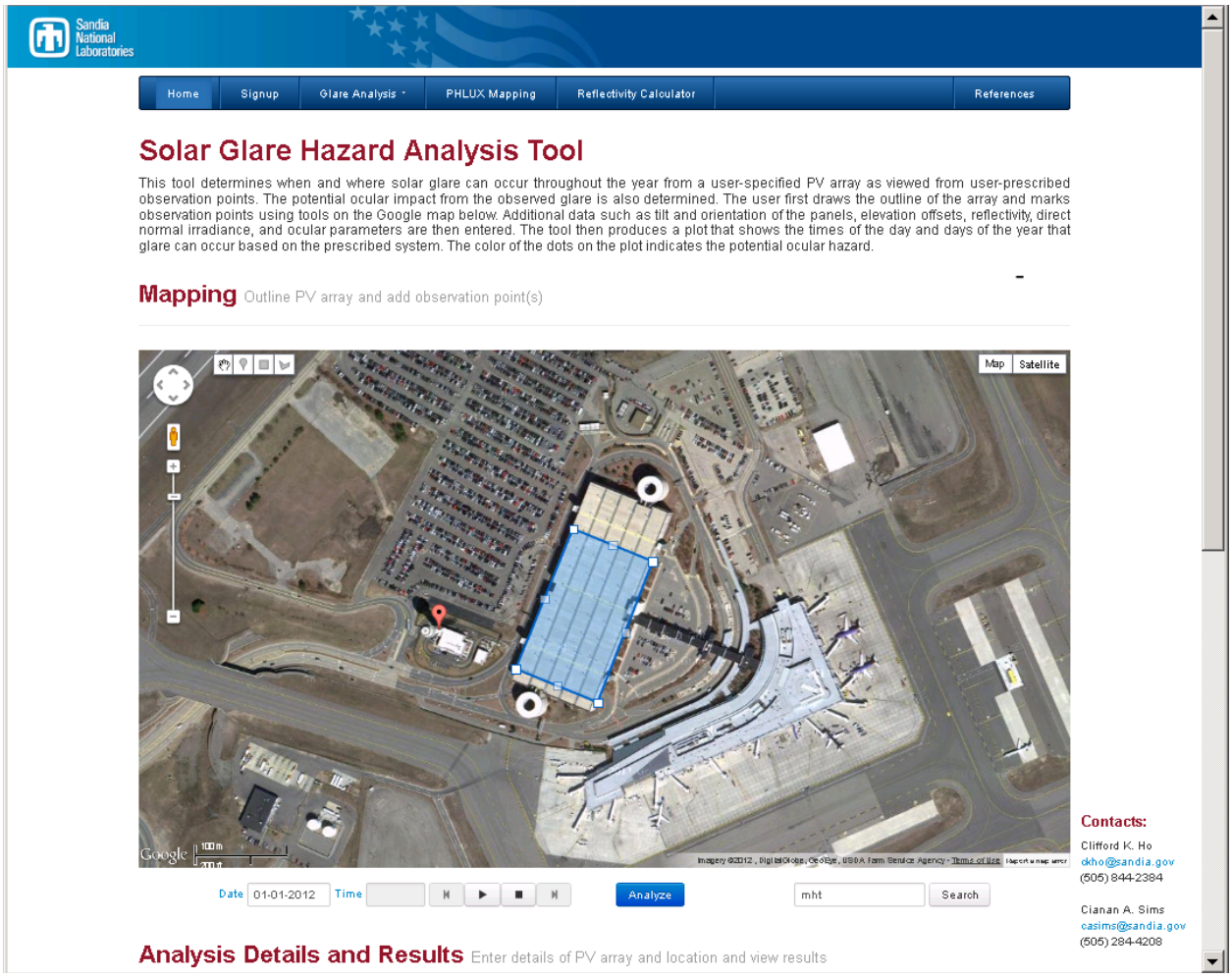

Figure 6. Screen image of glare analysis of the Manchester Boston Regional Airport. PV array (blue outline) and observation point (red marker) are entered using drawing tools integrated with Google Maps.

Figure 7 shows other input parameters entered by the user, including orientation and tilt of the PV array, elevations, rated power (for energy production calculations), optical and ocular parameters. The latitude, longitude, and elevation coordinates of the user-drawn PV array and observation points are automatically calculated in Google Maps and used to determine sun position and vector calculations for the glare and energy production analyses.

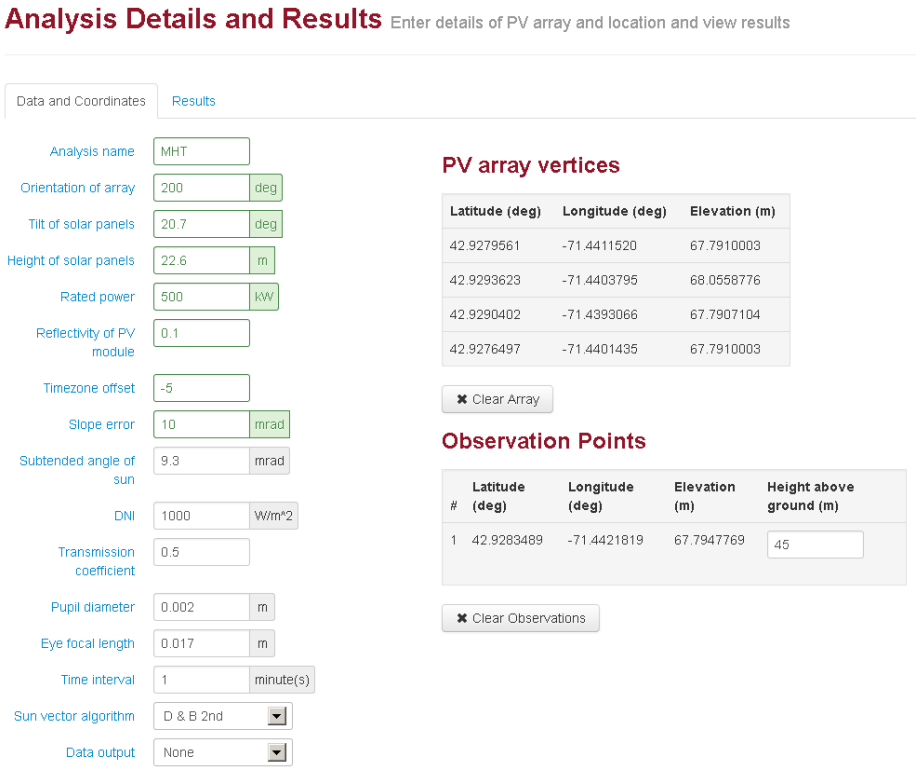

Figure 7. Input parameters used in SGHAT for glare analysis at MHT.

Figure 8 and Figure 9 show the results of the glare analysis assuming different values for the optical slope error of the PV modules, which impacts the scatter and beam spread. The dots in the plot represent occurrences of glare as viewed from the user-specified observation point relative to the specified PV array as a function of the time of day and day of the year. The color of the dots indicates the potential ocular hazard, which is impacted by the direct normal irradiance, optical parameters (reflectance, slope error/scatter), and ocular parameters (pupil diameter, transmission coefficient, ocular focal length). In Figure 8 and Figure 9, there is a potential for glare that can cause temporary after-image (a lingering image of the glare in the field of view) during the early morning. Assuming a zero optical slope error predicts that no glare will be visible from the end of November to mid-January. Assuming an optical slope error of 10 mrad, which yields a total beam spread of the reflected glare image of 0.13 rad (~7 degrees), predicts that glare will be visible all year.

An animation tool in SGHAT allows users to view the location of the observed glare at various times throughout the year when glare is predicted to occur. At MHT, the general spatial and temporal pattern of glare is shown in Figure 10.

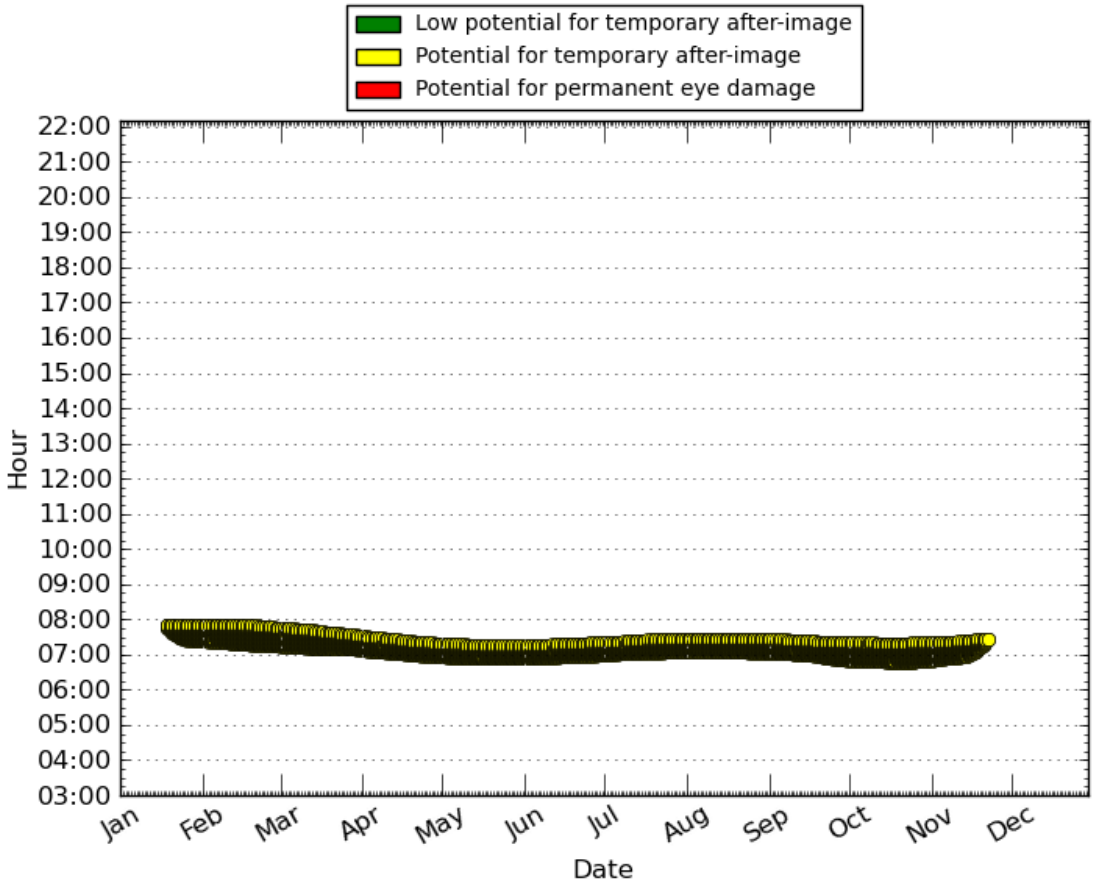

Figure 8. Plot showing when glare can occur (time and date) and the potential for ocular impact (represented by the color of the dots) in the ATCT assuming an elevation of 45 m above ground level with an optical slope error of 0 mrad (beam spread of 0.0093 rad, which is the subtended angle of the sun). Times are Eastern Standard Time (during Daylight Savings Time, add one hour).

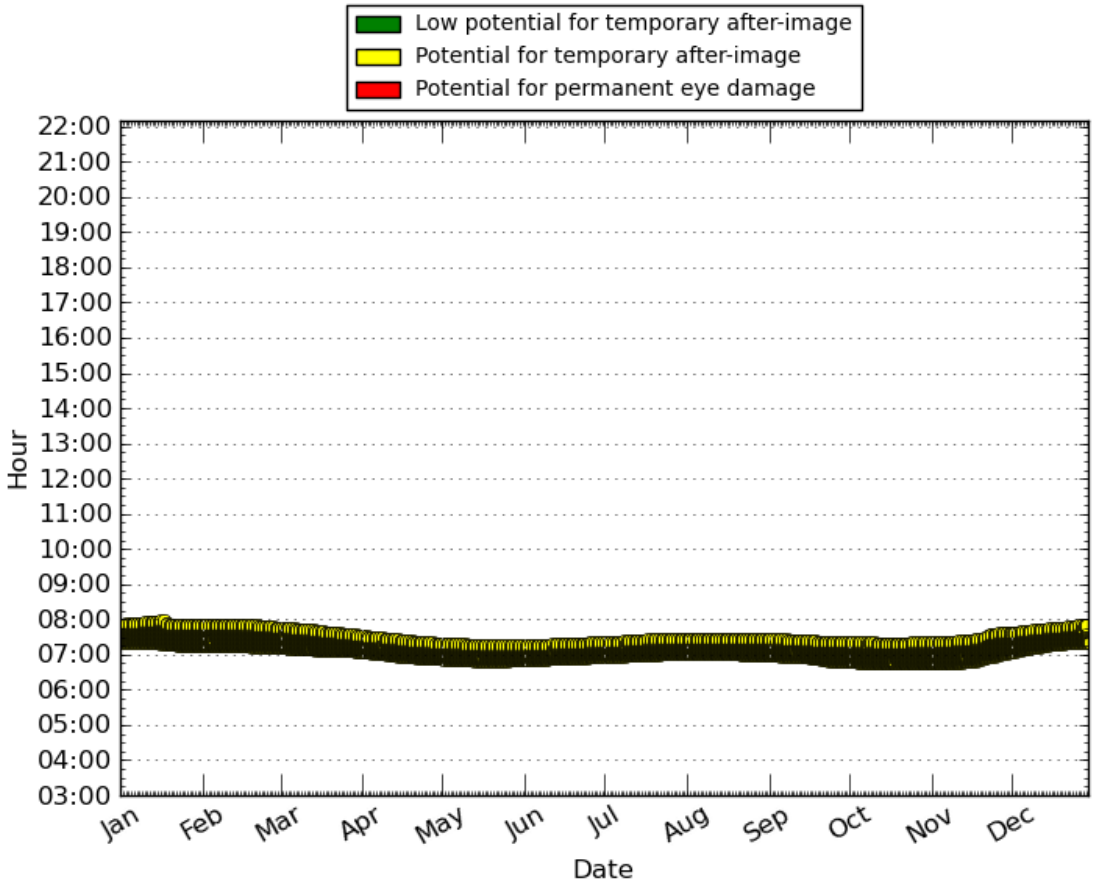

Figure 9. Plot showing when glare can occur (time and date) and the potential for ocular impact (represented by the color of the dots) in the ATCT assuming an elevation of 45 m above ground level with an optical slope error of 10 mrad (beam spread of 0.13 rad or ~7 degrees). Times are Eastern Standard Time (during Daylight Savings Time, add one hour).

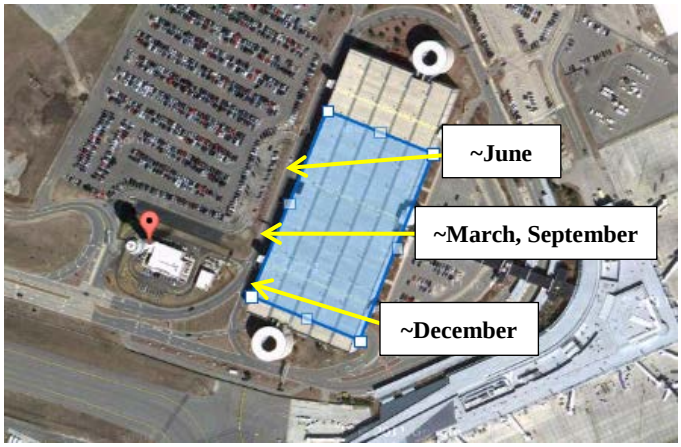

Figure 10. Approximate predicted locations and movement of glare on PV array at various times of the year.

Photos and videos of glare from the installed PV array at MHT were taken from the Air Traffic Control Tower in late April and early May. Glare was observed during hours that were consistent with those predicted by the glare tool (see Figure 11 and Figure 12; note that the hours shown in the ocular hazard plot in Figure 8 and Figure 9 are Eastern Standard Time, but the times shown in the photos in Figure 11 and Figure 12 are Eastern Daylight Time). Because of the glare, tarp was placed over the offending PV modules.

Features such as gaps between modules, uncertainty in the relative height of the PV modules and observation points, obstructions/land features between the PV array and the observation point, uncertainty in the optical properties of the modules, and atmospheric attenuation may impact the actual perception and time of observed glare.

Figure 11. Glare viewed from Air Traffic Control Tower at Manchester/Boston Regional Airport (8:15 AM EDT, 4/27/12).

Figure 12. Glare viewed from Air Traffic Control Tower at Manchester/Boston Regional Airport (~8:17 AM EDT, 5/10/12). Note that tarp has been placed over some of the modules.

The Solar Glare Hazard Analysis Tool can also be used to predict the relative energy production from alternative configurations (orientation, tilt, etc.) so that designs can be identified that not only mitigate glare but also maximize energy production. Table 1 shows alternative configurations using the same footprint of the PV array shown in Figure 6 that are predicted to produce no glare. The relative annual energy production is also shown for each configuration. In addition, the current PV configuration (200° azimuthal angle, 20.6° elevation angle) and a maximum energy production configuration (180° azimuthal angle, 43° elevation angle) are shown in Table 1. The optimal configuration using the same footprint that is predicted to produce no glare to the ATCT while maximizing energy production employs an azimuthal angle of 120° and an elevation angle of 40°.

Table 1. Alternative PV array configurations that are predicted to produce no glare to the ATCT (unless otherwise noted). Azimuthal angle is measured clockwise from due north (0°); elevation angle is measured from 0° (facing up) to 90° (facing horizontal). Note: these analyses assumed an ATCT cabin elevation of 51.2 m, which was provided by HMMH. We were informed later that the cabin elevation was lower (~45 m), so other configurations with no glare to the ATCT may be possible (e.g., Az=110°, El=20.6°).

Azimuthal Angle (degrees)	Elevation Angle (degrees)	Relative Annual Energy Production
180	43	100.0%*
200	20.6	93.9%**
120	40	88.9%
120	50	87.2%
110	30	85.0%
110	40	84.7%
120	60	83.7%
110	50	82.8%
130	70	81.5%
100	30	80.9%
100	20	80.8%
100	40	79.9%
110	60	79.3%
120	70	78.3%
100	50	77.6%
90	20	77.5%
210	80	76.9%
90	30	76.4%
220	80	75.8%
90	40	74.5%
110	70	74.2%
100	60	74.1%
130	80	74.0%
90	50	71.8%
120	80	71.3%
100	70	69.2%
90	60	68.1%
110	80	67.7%
90	70	63.4%
100	80	63.2%
90	80	57.8%

*Maximum energy production; produces glare to ATCT
**Current configuration; produces glare to ATCT

Based on a review of the glare analyses, an alternative configuration of the PV modules was recommended where the assemblies are rotated 90° counter-clockwise so that they are facing

toward the east-southeast (110° from due north). The tilt of the modules remains the same (however, since the downward tilt of the roof is 1.2° from east to west (e-mail from Rich Fixler on 11/16/12), the actual tilt of the modules is 20.7° - 1.2° = 19.5°.

Figure 13 shows a screen image of the SGHAT analysis with the PV array outlined in blue and the location of the ATCT indicated by the red marker. The input parameters used in the model are shown in Figure 14.

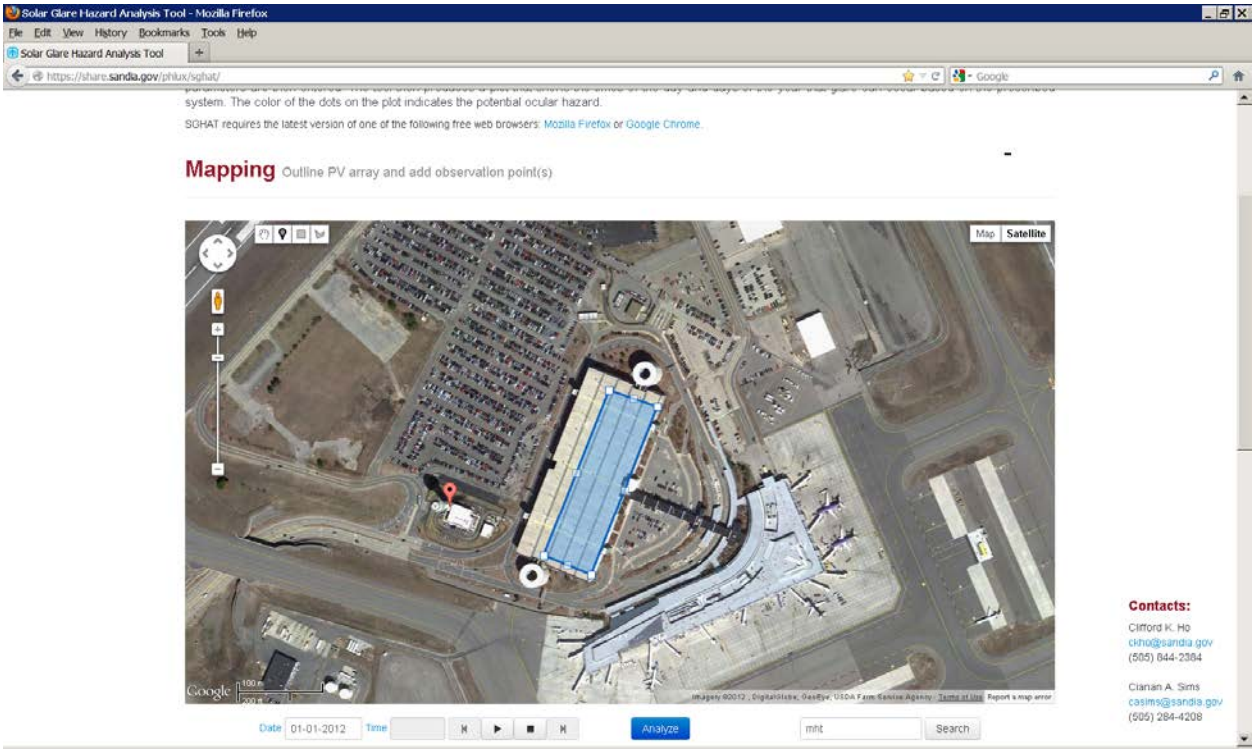

Figure 13. Location of alternative PV array configuration (outlined in blue) rotated 90° counter-clockwise so that they are facing toward the east-southeast (110° from due north).

In addition to the ATCT, observation points along straight approaches to runways 35, 6, 17, 24 were also evaluated. See Table 2 and Figure 15 – Figure 18 for locations and elevations of observation points along the approach to these runways.

For this new configuration (PV assemblies rotated 90° counter-clockwise), no glare was predicted to be observed in the ATCT or at the observation points along the approaches to runways 35, 6, and 17. It should be noted that the elevation of the ATCT observation point was varied between 40 – 51 m and no glare was predicted. Based on drawings of the ATCT tower, the elevation of the ATCT cabin is ~45 m.

Glare was predicted to be observable during final approach to runway 24 at locations between 2 km to 5 km from touchdown during winter months in the afternoon (for up to a few minutes on each day that glare was predicted to occur). Figure 19 – Figure 22 show the specific dates and times that glare was predicted to occur at these observation points. However, the model

predicted that there was a low potential for ocular impact at all locations that glare was predicted to occur.

The annual energy produced from this new configuration was predicted to be within ~1% of the existing configuration. The existing configuration consists of 2210 modules with a rated power capacity of ~530 kW (~240 W/module). The new configuration has 247 additional modules for a rated power capacity of ~589 kW. Using these values, SGHAT predicts that the maximum annual energy production for the existing and new designs are 1.30 GWh and 1.29 GWh, respectively, assuming clear-sky conditions and constant direct normal irradiance (DNI) of 1,000 W/m^2 all year. Actual annual energy production will be less due to variable (lower) DNI in the mornings and evenings and when the sky is cloudy. Future versions of SGHAT will incorporate variable DNI values representative of a typical meteorological year for specific sites.

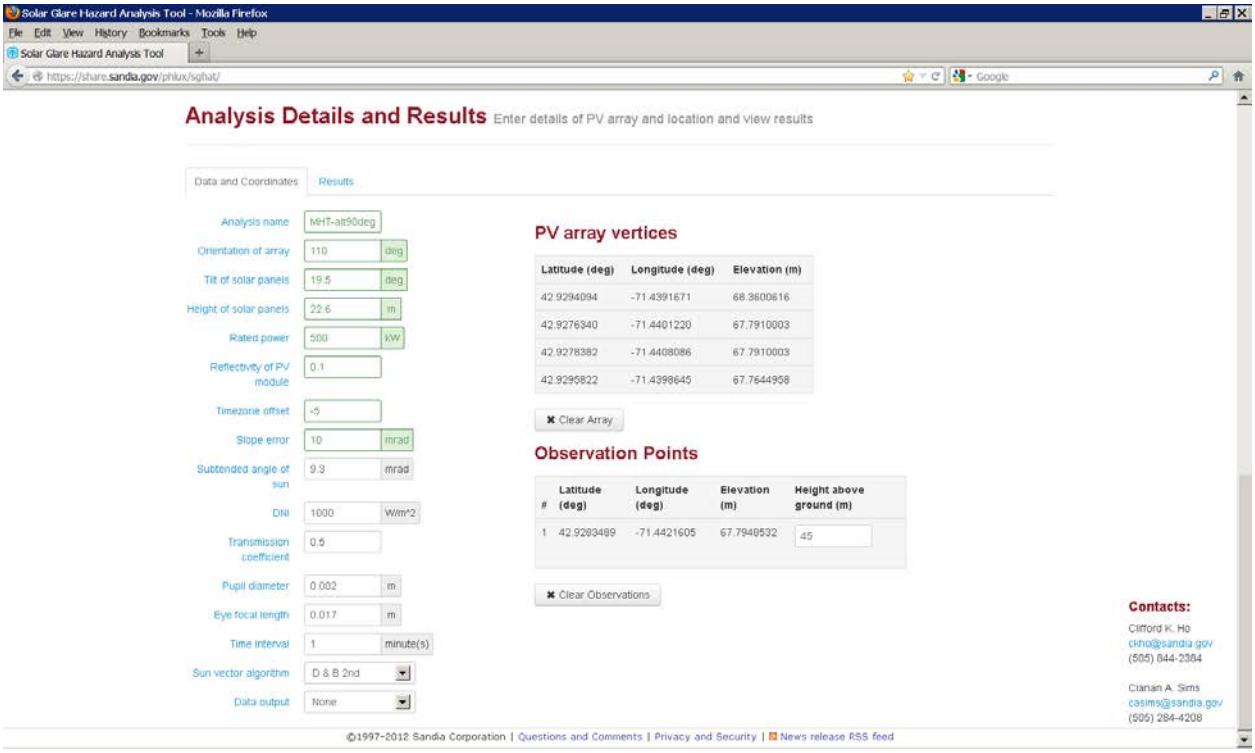

Figure 14. Input parameters used in SGHAT analysis. Observation point is for the ATCT (observation points change for different runway approaches).

Table 2. Observation points for straight approaches to runways 35, 6, 17, and 24.

Observation Point #	Description	Dist. From Landing Location (m)	Elevation (m)
1	Touchdown (TD)	0	0
2	Threshold Point	300	15.72
3	1 km from TD	1000	52.41
4	2 km from TD	2000	104.82
5	3 km from TD	3000	157.22
6	4 km from TD	4000	209.63
7	5 km from TD	5000	262.04

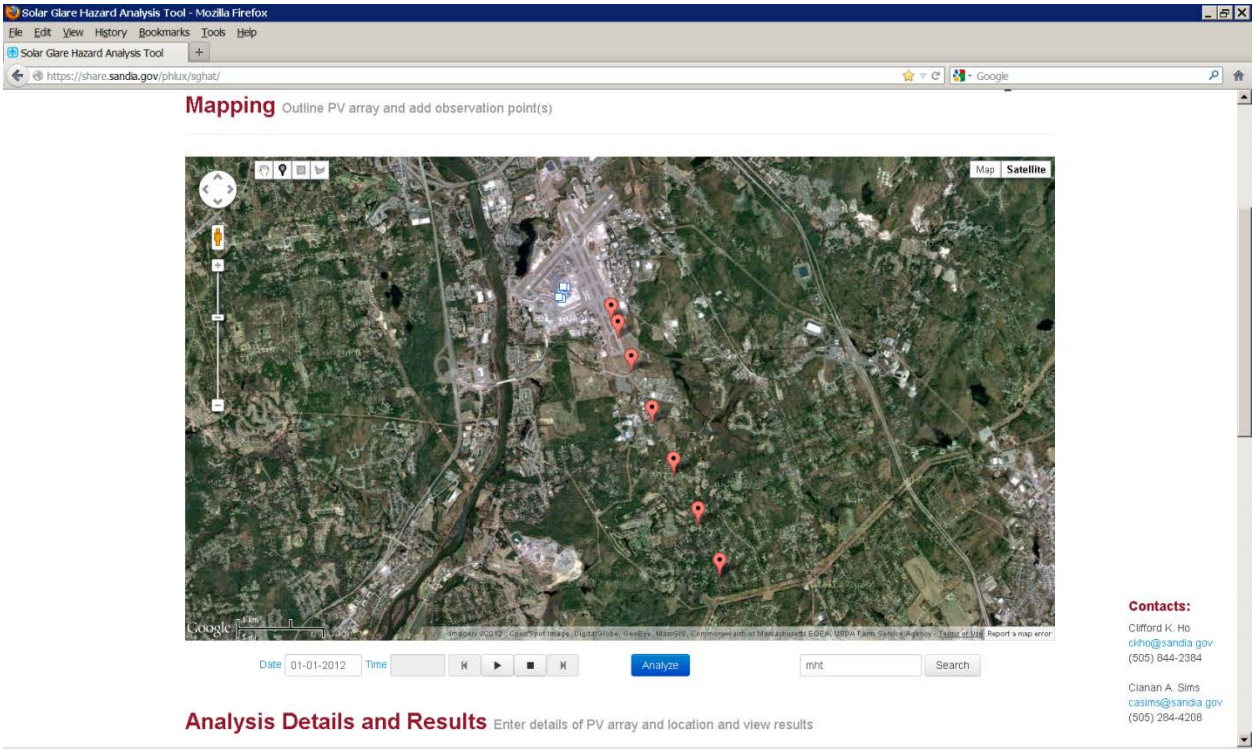

Figure 15. Observation points approaching Runway 35 from the southeast.

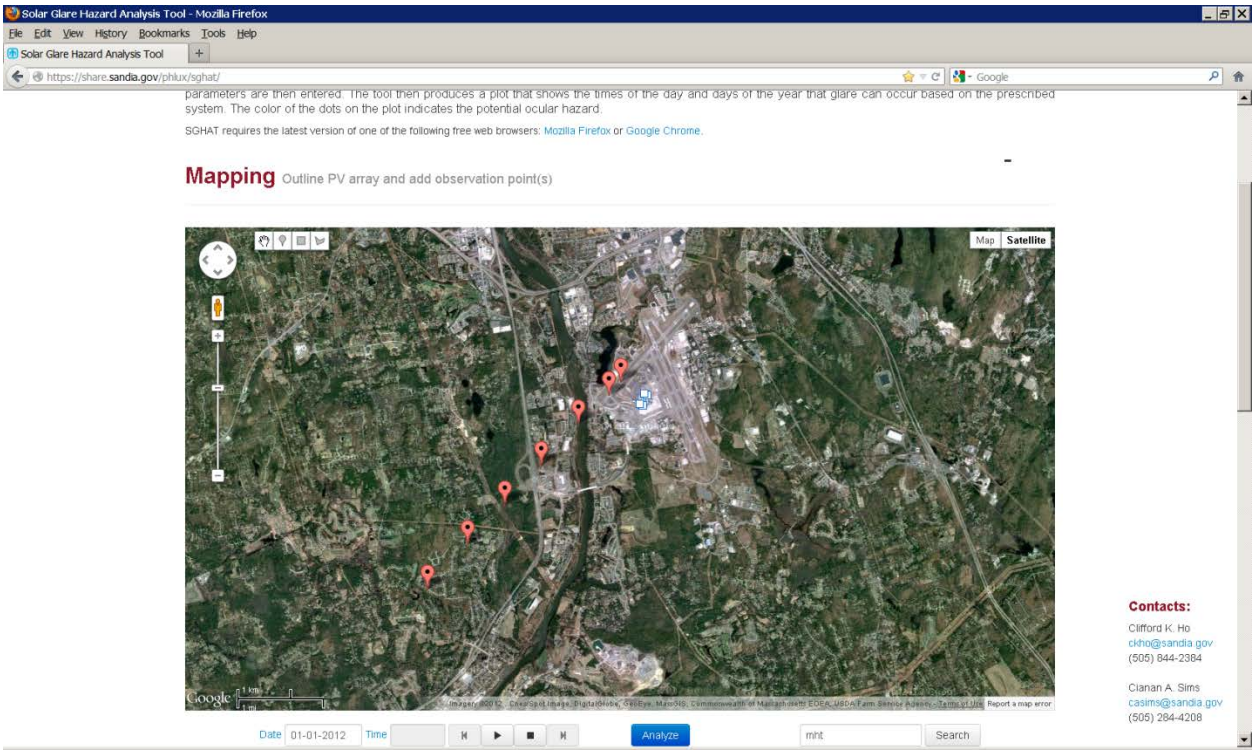

Figure 16. Observation points approaching Runway 6 from the southwest.

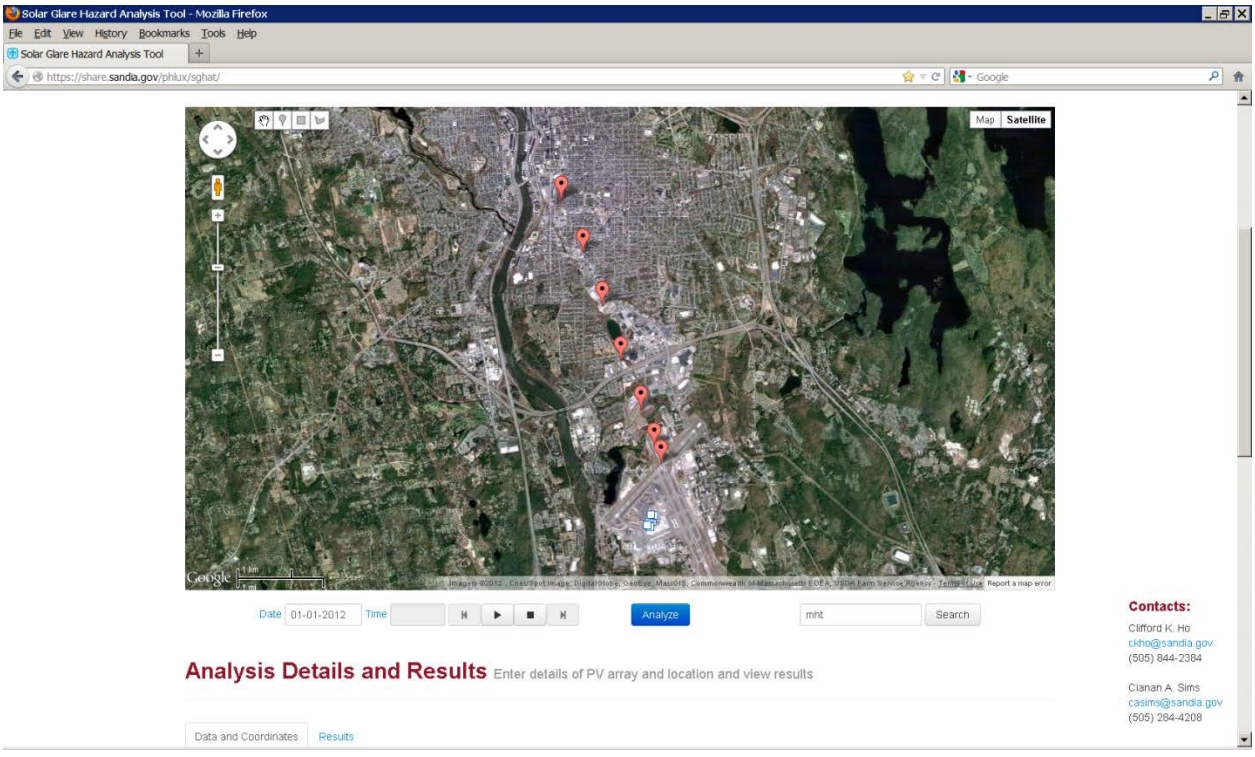

Figure 17. Observation points approaching Runway 17 from the northwest.

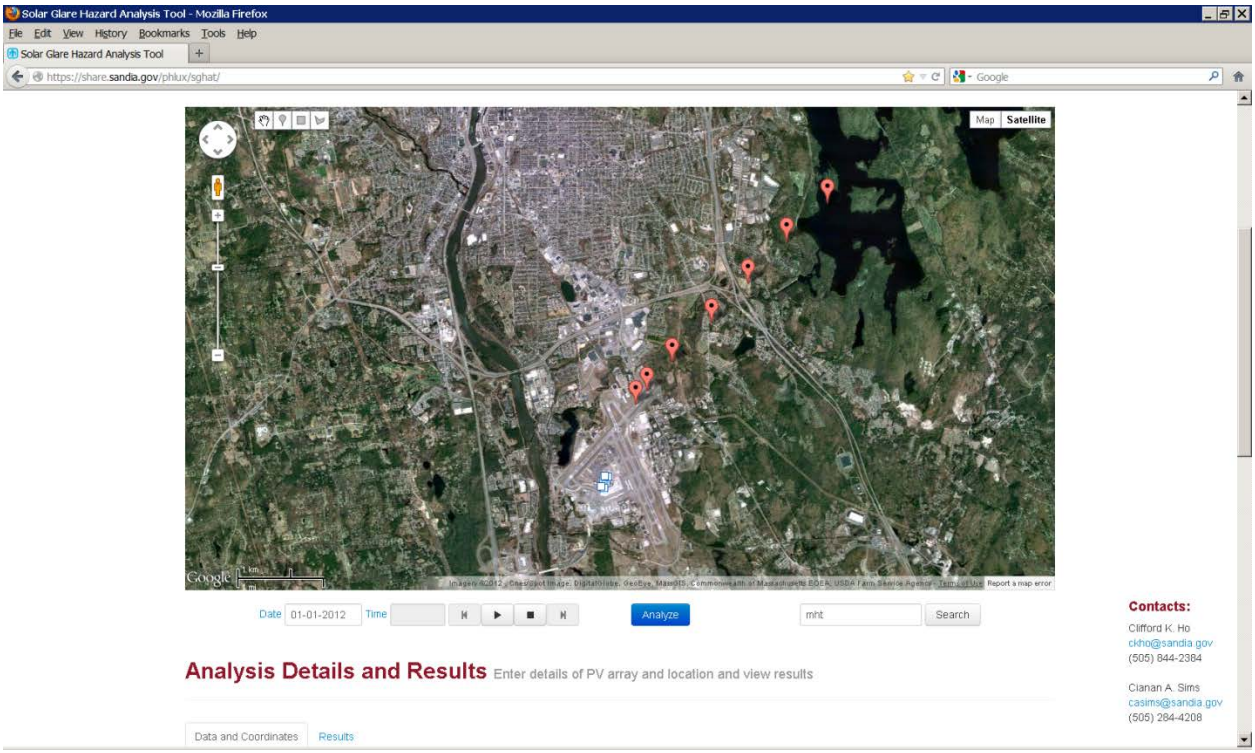

Figure 18. Observation points approaching Runway 24 from the northeast.

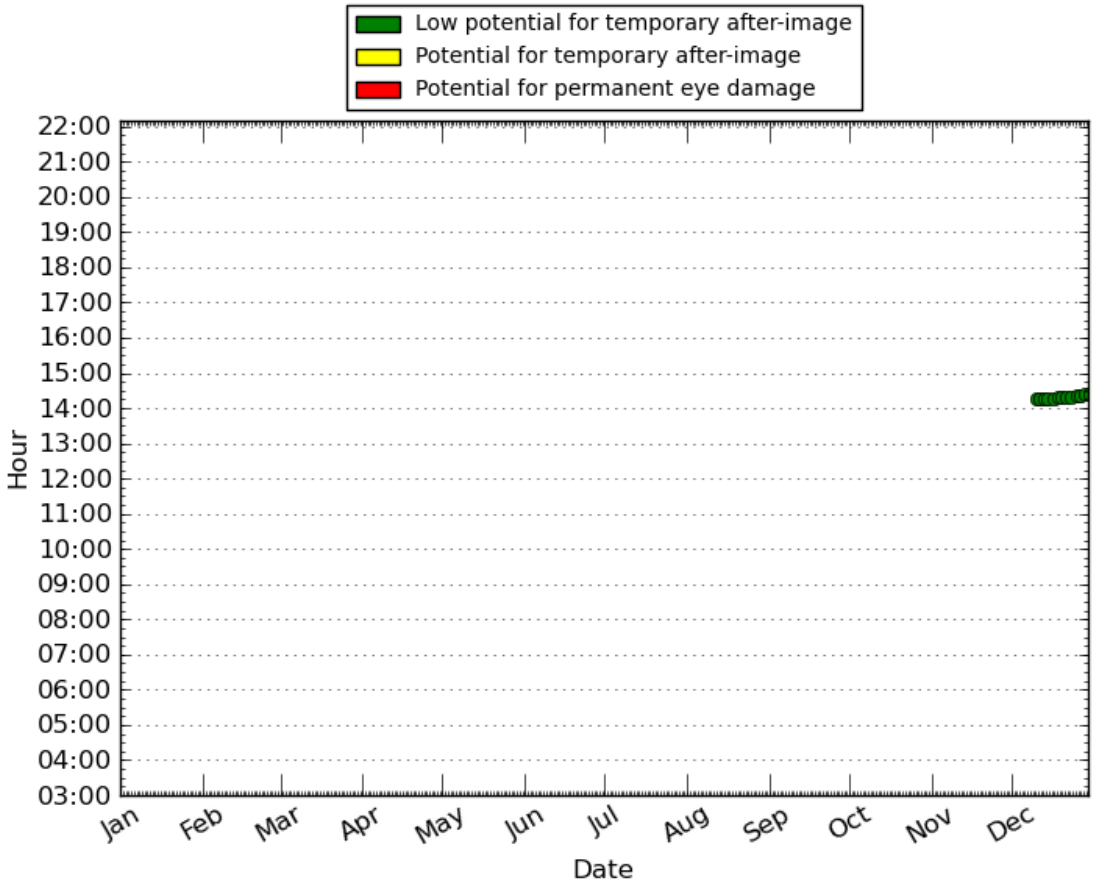

Figure 19. Predicted glare and potential ocular hazard from observation point 4 (2 km from touchdown) on approach to Runway 24. A low potential for ocular impact is predicted.

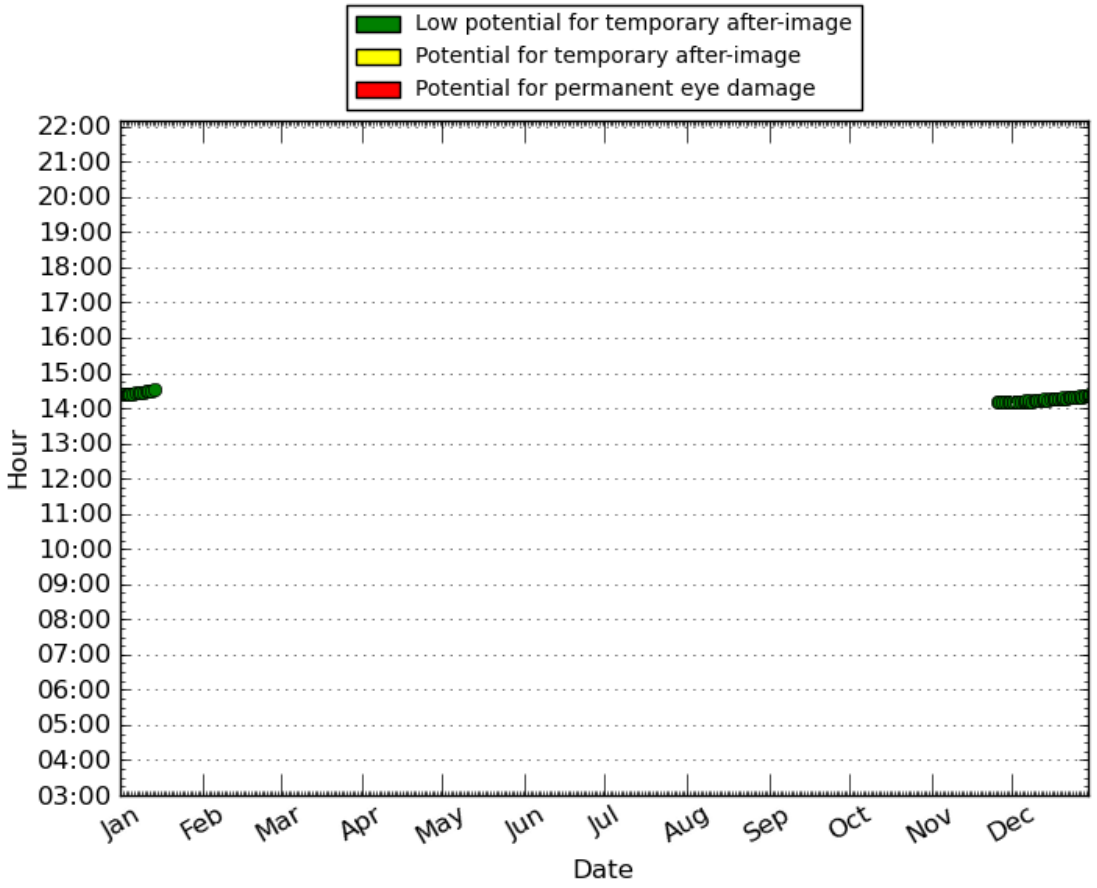

Figure 20. Predicted glare and potential ocular hazard from observation point 5 (3 km from touchdown) on approach to Runway 24. A low potential for ocular impact is predicted.

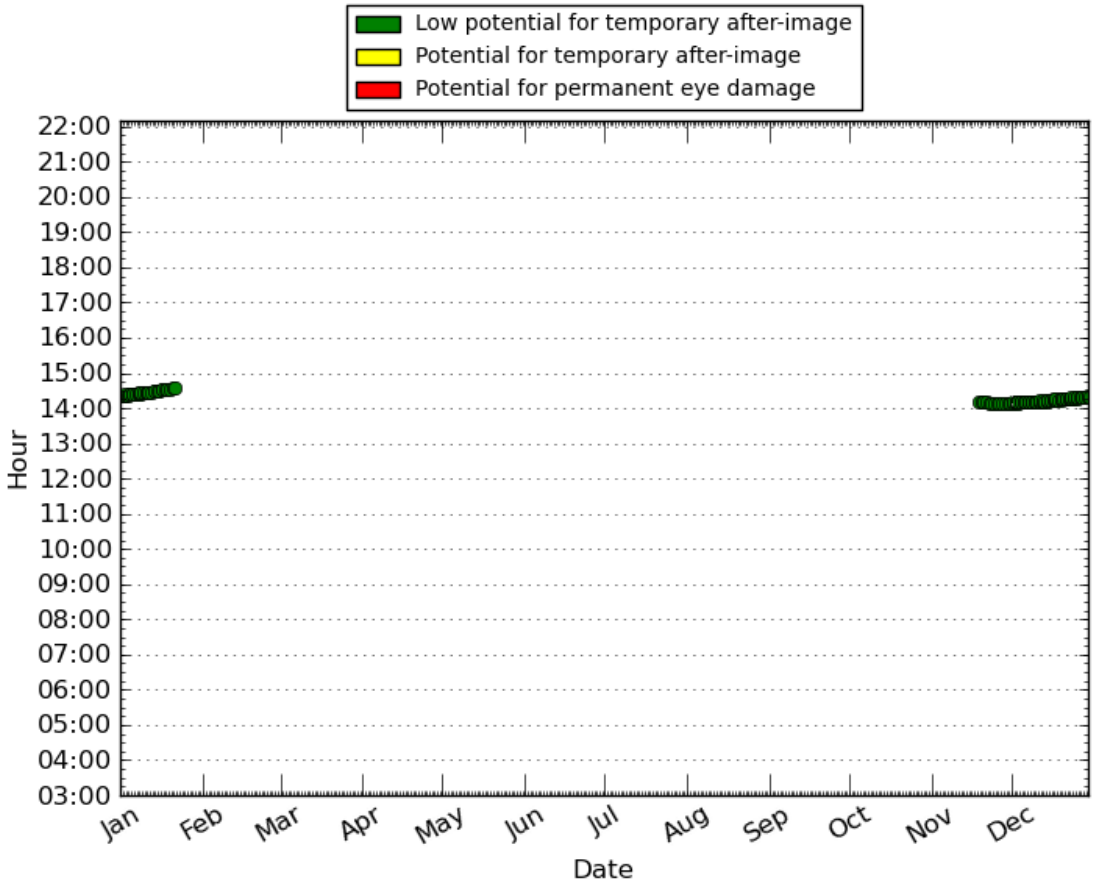

Figure 21. Predicted glare and potential ocular hazard from observation point 6 (4 km from touchdown) on approach to Runway 24. A low potential for ocular impact is predicted.

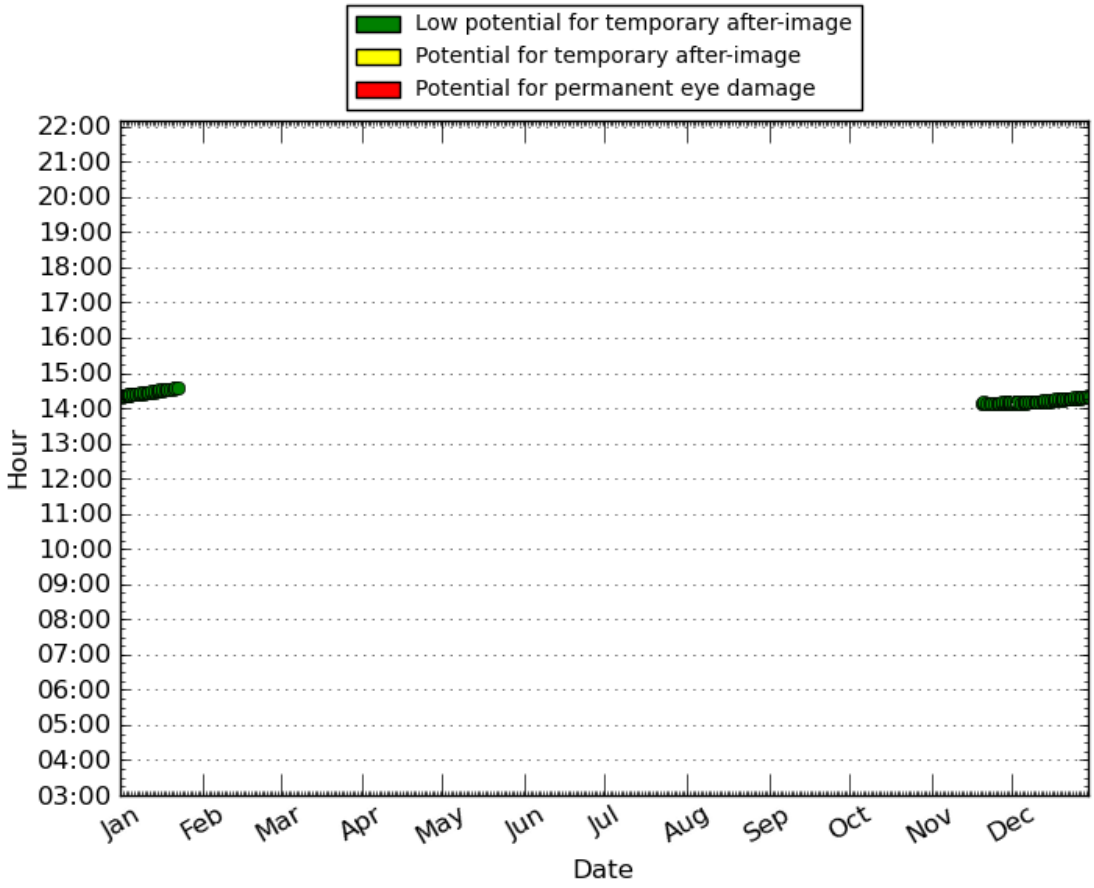

Figure 22. Predicted glare and potential ocular hazard from observation point 7 (5 km from touchdown) on approach to Runway 24. A low potential for ocular impact is predicted.

7. Acknowledgments

Sandia National Laboratories is a multi-program laboratory managed and operated by Sandia Corporation, a wholly owned subsidiary of Lockheed Martin Corporation, for the U.S. Department of Energy's National Nuclear Security Administration under contract DE-AC04-94AL85000.

8. References

[1] Ho, C.K., C.M. Ghanbari, and R.B. Diver, 2011, Methodology to Assess Potential Glint and Glare Hazards From Concentrating Solar Power Plants: Analytical Models and Experimental Validation, *Journal of Solar Energy Engineering-Transactions of the Asme*, **133**(3).

[2] Sliney, D.H. and B.C. Freasier, 1973, Evaluation of Optical Radiation Hazards, *Applied Optics*, **12**(1), p. 1-24.

Additional references can be found at www.sandia.gov/glare.